

Torsion-induced fluorescence quenching in excited-state intramolecular proton transfer (ESIPT) dyes

Sehoon Kim¹, Jangwon Seo, Soo Young Park*

Organic Nano-Photonics Laboratory, School of Materials Science and Engineering, Seoul National University, San 56-1, Shillim-dong, Kwanak-ku, Seoul 151-744, Republic of Korea

Received 28 October 2006; received in revised form 28 February 2007; accepted 23 March 2007

Available online 30 March 2007

Abstract

Fluorescence quenching behaviors of four known excited-state intramolecular proton transfer (ESIPT) molecules have been studied by semiempirical and ab initio calculations. The ESIPT compounds studied in this work are assorted into two sets depending on the N-containing ring structure (5- and 6-membered rings). It has been found that twisted intramolecular charge transfer (TICT) process in the excited keto state (K^*) after ESIPT, one of the possible quenching pathways of ESIPT fluorescence, is significantly influenced by the geometrical properties of intramolecular hydrogen (H) bond associated with the N-containing ring structure. The compounds with 5-membered ring have efficient ESIPT emission with large barrier to fluorescence-quenching TICT state, due to appropriate stabilization of planar K^* through intramolecular H bond. For the compounds with 6-membered ring, however, ESIPT emission is completely quenched due to significantly lowered barrier resulting from too short H-bond length. The effect of intramolecular H bond on the TICT reaction potential has been discussed in detail from the viewpoints of molecular structure and torsional motion, with the help of elaborate model compound studies.

© 2007 Elsevier B.V. All rights reserved.

Keywords: Twisted intramolecular charge transfer (TICT); Intramolecular hydrogen bond; Excited-state intramolecular proton transfer (ESIPT); Fluorescence quenching; Semiempirical and ab initio calculations

1. Introduction

Luminescence-based applications, one of the most important and promising topics in materials science, have led to great development of fluorescent and phosphorescent molecules. Since the luminescent properties of molecules are key factors governing application features, understanding and control of radiative and nonradiative decay processes are not only demanded to optimize the existing performance, but also expected to encourage novel and innovative application concepts. Recently, fluorescent molecules capable of luminescence change responsive to molecular environment, are gaining great interest for their potential applications from typical polarity and viscosity probes [1] to more advanced ones including biosensors [2], logic gates [3], and optical recordings [4]. Aggregation-triggered turn-on luminescence switching of nonfluorescent

molecules is a more recent and special example, where environment change from isolated monomer to concentrated aggregate blocks nonradiative deactivation path of the first excited singlet state (S_1) to generate fluorescence [5–7].

As another candidate for luminescence on-off switching and viscosity probe, we have reported a novel 2-(2'-hydroxyphenyl)quinoline-based excited-state intramolecular proton transfer (ESIPT) molecule (HPQ, see the structure in Fig. 1a and b), and its polymeric and dendritic derivatives, which have successfully been utilized for their applications to electroluminescence, solid-state lasing, and fluorescence recording [4,8–12]. These HPQ-related molecules are nonfluorescent (monomers and dendrimers) or weakly fluorescent (main-chain polymers) in solution but orange fluorescent in solid states such as crystals, amorphous glass, and polymer blend films. ESIPT is a photoinduced enol-to-keto tautomerization via proton transfer in the excited state. Several mechanisms for nonradiative transition of ESIPT molecules have been proposed but still unproven. According to the literature [13,14], the twisted intramolecular charge transfer (TICT) reaction in the excited-state keto form, which is accessed after ESIPT, is one of the possible reasons for

* Corresponding author. Tel.: +82 2 880 8327.

E-mail address: parksy@snu.ac.kr (S.Y. Park).

¹ Present address: Institute for Lasers, Photonics and Biophotonics, University at Buffalo, The State University of New York, Buffalo, NY 14260-3000, USA.

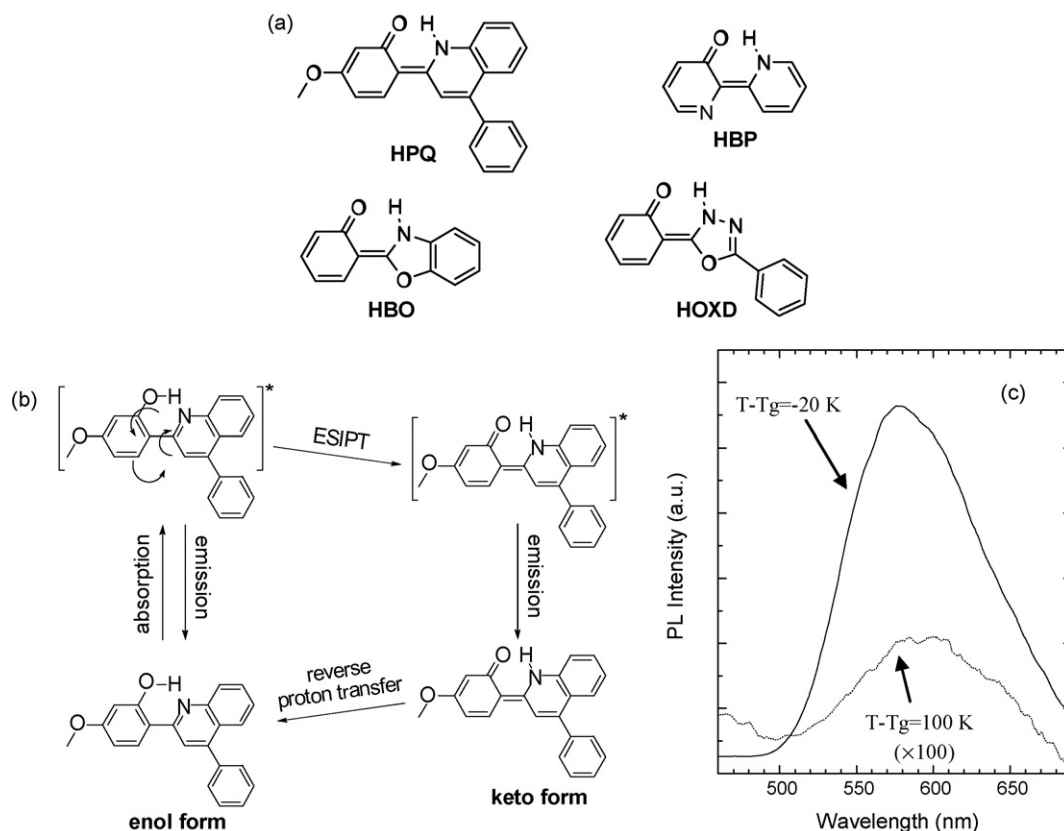


Fig. 1. (a) Keto forms of ES IPT compounds studied in this study. (b) Four-level photochemical and photophysical processes of phototautomerizable HPQ. (c) Photoluminescence (PL) spectra of HPQ doped in polymeric medium ($T_g = 40^\circ\text{C}$) at different temperatures, excited at 370 nm. Dotted line is magnified 100 \times for clarity, where the shoulder below 500 nm is a background signal from glass slides of the sandwich cell.

the fluorescence quenching observed in solution. Accordingly, the fluorescence generation in the solid states is understood as the result from the prevented TICT by kinetic constraint which blocks large-amplitude twisting motion. TICT state often acts as an intramolecular fluorescence quencher due to the $n\pi^*$ characteristics or the much reduced S_0 – S_1 energy gap [15]. Polarity and hydrogen-bonding ability of the solvents also have profound influences on the emission behaviors of ES IPT compounds as well as on the ES IPT reaction itself, which are well-documented in the literature [16]. In this study, we focus on the TICT reaction as a post-ES IPT fluorescence quenching process in nonpolar, aprotic environments where the occurrence of ES IPT is not perturbed. We have investigated the TICT reaction in the proton-transferred excited keto form (K^*) of the representative ES IPT molecules (Fig. 1a), in terms of the molecular structure and torsional motion in the S_1 state by utilizing gas-phase molecular orbital calculations. A guideline for molecular design has been deduced in terms of the structural effects of ES IPT molecules on TICT-induced fluorescence quenching.

2. Experimental

Synthetic details of HPQ are described in the literature [4]. Viscosity-dependent fluorescence change of HPQ were measured in a poly(methyl methacrylate) (PMMA) mixture containing appropriate amount of plasticizer, benzyl phthalate

(BBP), to give the glass transition temperature (T_g) at 40°C . The chloroform solution of PMMA mixture with 1 wt% of HPQ was cast onto a glass slide, completely dried, and sandwiched with the second glass slide at a certain temperature above T_g , using 25 μm -thick polyimide film as a spacer. Temperature-dependent photoluminescence spectra were measured on a fluorescence spectrophotometer (Shimadzu, RF-5301PC) with the sandwiched sample attached to a vertical hot plate.

Semiempirical (pm3) and ab initio (6-21G) calculations were performed in gas phase using Mopac 2000 (Fujitsu), HyperChem 7.5 (Hypercube), and PC GAMESS (Version 6.3). The geometries of ES IPT molecules and a model compound, 3-aminoacrylaldehyde, were optimized in the ground state (S_0) without any structural constraints. Geometry-dependent potential energies in the S_0 and the S_1 states were calculated by changing geometrical parameters of interest from the optimized geometry. The model structure, 6-aminomethylene-cyclohexa-2,4-dienone in Fig. 4a, was optimized at every geometry point with restraint of θ at the 3-21G level, using HyperChem. The S_1 state energies at the 6-21G level were calculate using GUGA CI code implemented in PC GAMESS.

3. Results and discussion

Fig. 1b shows the four-level cyclic photoreaction scheme of HPQ. ES IPT is an excited enol (E^*)-to-excited keto (K^*) tau-

tomization triggered by photoexcitation of intramolecularly hydrogen-bonded enol (E) tautomer which is a main species populating the ground state. After radiative decay from K^* to K, subsequent ground-state reverse proton transfer regenerates the initial E form, bringing the reaction cycle to completion ($E \rightarrow E^* \rightarrow K^* \rightarrow K \rightarrow E$). ESIPT molecules with efficient keto emission have been widely exploited as proton-transfer laser dye, solar concentrator, and polarity probe, etc., due to the negligible self-absorption by large Stokes' shift arising from different absorbing (E) and emitting (K^*) species. Particularly, HPQ derivatives in the solid state have wide application potentials as ESIPT molecules with large Stokes'-shifted (10413 cm^{-1}) keto emission at 580 nm. In solution, however, they show complete quenching of keto emission very peculiarly. This feature, on the other hand, offers a unique viscosity probing ability, as shown in Fig. 1c. The emission intensity of polymer-dispersed HPQ is gradually increased ca. 320 times by temperature decrease from $T-T_g$ of 100 to -20 K .

To gain an insight into the molecular-level origin of HPQ's fluorescence quenching, potential energy surfaces of enol and keto forms were calculated semiempirically in isolated gas phase as a function of certain dihedral angles of interest. The gas-phase result in Fig. 2a indicates that the enol form in the ground state prefers the H-bonded planar conformation owing to the resonance-assisted hydrogen bond (RAHB) stabilization [17]. This predetermined planar geometry is known to be most favorable for ESIPT via intramolecular H bond, suggesting that ESIPT in HPQ should be quite efficient even in solution with minimal viscosity. Actually, no observable enol emission from HPQ in both solution and solid states indicates that, regardless of environment viscosity, the E^* form decays exclusively to the K^* form by efficient ESIPT rather than radiatively to the E form. Therefore, it is deduced that the emission quenching of HPQ in solution is related with K^* formed after ESIPT. Fig. 2b is the potential energy curves of keto form in the ground (K) and the excited (K^*) singlet states with respect to the torsional angle around the central ethene ($C=C$) bond. Similar to the enol form, the optimized geometry in the ground state is H-bonded planar

conformation, which is no more the case for the excited state. The K^* form shows a deep energy well at the orthogonal conformation and two peaks at planar ones (0° and 180°). Around the H-bonded planar conformation at 0° , the peak height is lower than the other and a shallow local well is observed probably because the H-bond stabilization is still valid even in the K^* state. It is noted that the initially formed K^* would be near the H-bonded position at 0° because ESIPT occurs in the H-bonded planar E^* . Accordingly, just after ESIPT, one can expect easily accessible $C=C$ bond torsion, leading to the nonfluorescent orthogonal state. Since the keto form is an ethene derivative, this K^* state process is explained as TICT in asymmetrically substituted ethenes which has been well documented in the literature [15].

The effect of intramolecular H bond on TICT process was examined with the S_1 -state rotational potential curves around the $C=C$ bond of a simple model structure, 3-aminoacrylaldehyde [18], obtained at the 6-21G level. Depending on the orientation of carbonyl group, the model compound exists in two conformers of non-H-bonded transoid and H-bond-forming cisoid (Fig. 3a), where the latter represents the ESIPT keto tautomer. Regardless of the existence of H bond, both conformers in the S_1 state commonly have TICT-like twisted global minima with an energy dip at 90° and two peaks at *cis/trans* planar conformations (0° and 180° , respectively). Their lowest unoccupied molecular orbital (LUMO) diagrams in Fig. 3b shows the existence of node at $C=C$ bond, representing anti-bonding character and thus torsion feasibility in the S_1 state. In addition, the typical characteristics of TICT, i.e., the torsion-coupled charge transfer are clearly observed: the π -electron redistribution on LUMO and the resulting dipole moment change in the S_1 state during the orthogonal distortion. It is importantly noted that the peak energy of H-bonded *cis-cisoid* conformer is significantly lowered over other planar conformation without H bond *trans-cisoid*, strongly supporting the role of H-bond stabilization in the TICT potential modulation. As a result, H-bond-forming *cisoid* conformer has an asymmetric potential curve similar to that of HPQ in the K^* state having a shallow local minimum near 0° (Fig. 2b). This evi-

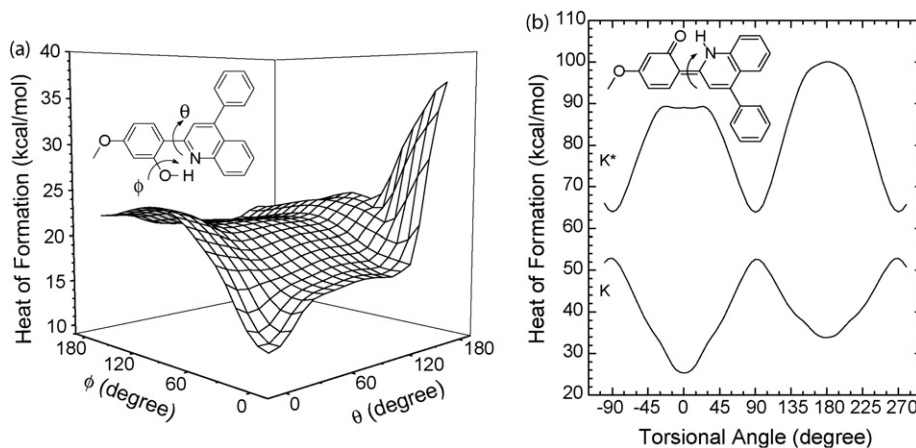


Fig. 2. (a) Potential energy surface (pm3) of HPQ enol form in the ground state (E) with respect to two rotational angles indicated in the structure. The inserted structure represents H-bonded planar conformation with $\phi = 0^\circ$ and $\theta = 0^\circ$. (b) Rotational potential curves (pm3) of HPQ keto form in the ground (K) and the first excited singlet (K^*) states with respect to the torsional angle around the central $C=C$ bond indicated in the inset structure.

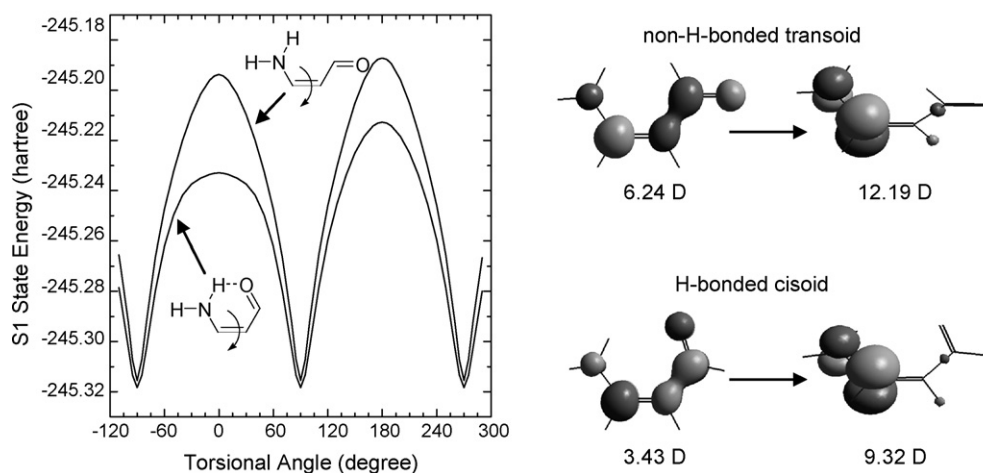


Fig. 3. (a) 3-Aminoacrylaldehyde conformers without (transoid) and with (cisoid) intramolecular H bond, and their rotational potential curves in the S1 state (6-21G) around the central C=C bond indicated in the inset structure. The inset structures represent a planar conformation with torsion angle of 0°. (b) Torsion-induced intramolecular charge separation represented by π -electron redistribution in LUMO and dipole moment change in the S1 state, obtained using pm3 formalism.

dences that TICT and H-bond stabilization are cooperative in the K^* state of ESIPT molecules to determine their emission properties. If H-bond stabilization is large enough to produce a deeper well at H-bonded planar peak potential, the increased rotational barrier height will block the competitive orthogonal distortion to the TICT state, leading to the increase in the efficiency of radiative decay from planar conformation.

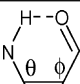
The effect of molecular structure on the magnitude of H-bond stabilization was examined with the known ESIPT molecules (Fig. 1a) which are classified by the structure of nitrogen-containing proton donor ring into 6-membered (HPQ and HBP) and 5-membered (HBO and HOXD) ones. The calculated geometry parameters and the fluorescence quantum yields of ESIPT emission are listed in Table 1. In spite of noticeable discrepancy between the geometrical data obtained by pm3 and 6-21G, the H-bond-related structure can be assorted by the N–C=C angle (θ) depending on the N-containing ring strain (5- or 6-membered). Due to larger inner angle, 6-membered rings result in smaller θ , which influences all other parameters, particularly H-bond angle (N–H...O) and length (O...H). Interestingly, fluorescence quantum yield is also correlated with these structural

parameters. ESIPT emission in nonpolar solvent is efficient for 5-membered molecules but quenched for 6-membered ones. This implies that the magnitude of H-bond stabilization is closely related with the N-containing ring structure of ESIPT molecules.

Fig. 4a shows the predicted effects of N-containing ring strain on the H-bond-related geometrical parameters and the S1 potential energy, obtained by using another model structure, 6-aminomethylene-cyclohexa-2,4-dienone. The ring strain effect was simulated by varying and fixing the N–C=C angle (θ) and optimizing the rest of the geometry at the 3-21G level. The N–C=C angle (θ) and the O...H distance are proportional to each other and optimal for H-bond stabilization at 125° and 1.80 Å, respectively. When compared with the 6-21G geometries of the ESIPT compounds (Table 1), these optimum parameters of the model structure are positioned between those for 5- and 6-membered compounds. In addition, two geometry points of the model structure in Fig. 4a ($\theta = 127^\circ$, O...H = 1.87 Å and $\theta = 111^\circ$, O...H = 1.54 Å) provide close proximity to the 5-membered and the 6-membered ESIPT compounds, respectively. With these two geometries as respective model structures

Table 1
Calculated geometrical parameters characterizing intramolecular H bond and fluorescence quantum yields (Φ_f)

Compound	Bond angle (°)				N–H...O ^a		O...H distance (Å) ^a		Φ_f
	θ^a		ϕ^a						
	pm3	6-21G	pm3	6-21G	pm3	6-21G	pm3	6-21G	
HPQ	119.7	119.71	121.7	119.2	132.5	144.3	1.78	1.55	0 ^b
HBP	118.5	117.5	122.6	119.7	134.1	147.0	1.78	1.48	0.001 ^c
HBO	125.1	126.9	118.1	116.9	124.3	129.7	1.84	1.78	0.03 ^d
HOXD	126.4	129.9	117.0	116.5	121.2	118.9	1.86	1.95	0.021 ^e

^a In the segment of , evaluated from the optimized keto forms in the ground state.

^b In cyclohexane. Not detectable in our measurement system.

^c From [13], in 3-methylpentane.

^d From [19], in methylcyclohexane.

^e From [20], in octane.

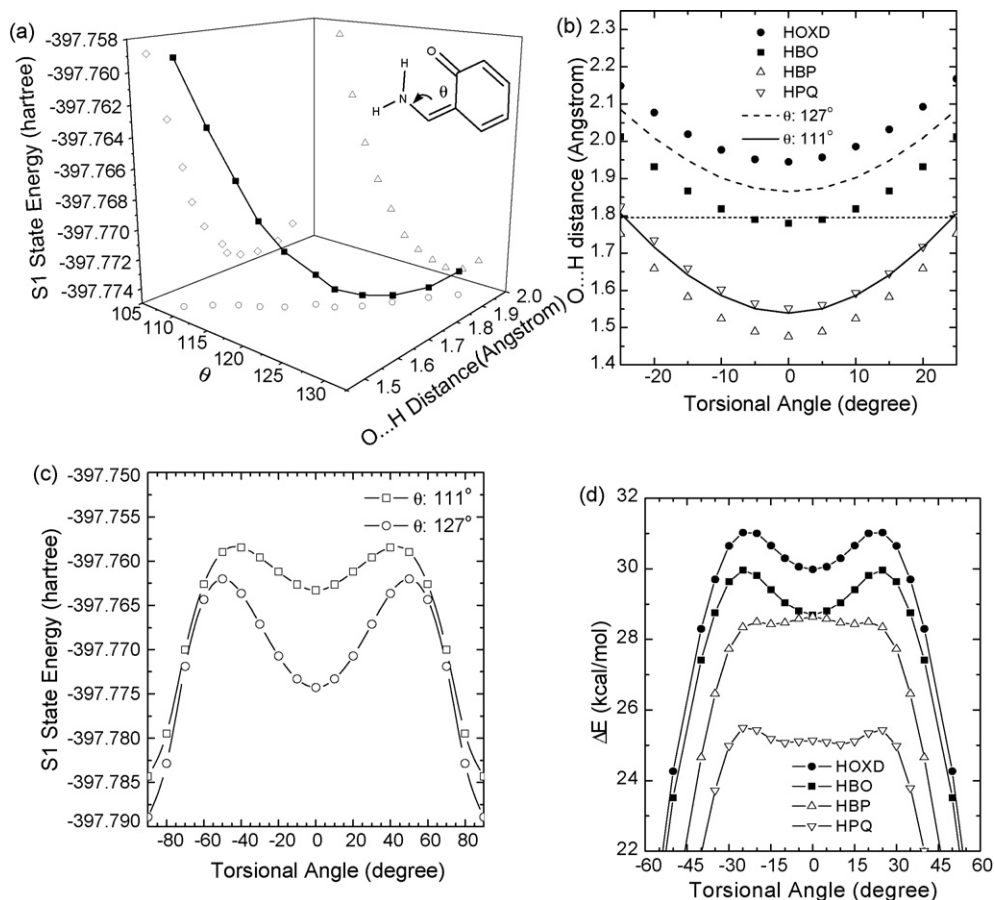


Fig. 4. (a) Effect of N–C=C angle (θ) on the O \cdots H bond length and the S_1 state energy (6-21G), evaluated from a model compound (6-aminomethylene-cyclohexa-2,4-dienone) which is optimized in the ground state with a restraint to varying θ values at the 3-21G level. Open symbols are projections on each plane. (b) Change in O \cdots H bond length during rotation around the central C=C bond of ESIPt compounds shown in Fig. 1a. Dotted line indicates the optimal O \cdots H bond length obtained from a. Dashed and solid curves are for the model compound with the indicated θ values. (c and d) Rotational potential curves around the central C=C bond in the S_1 state of the model compound with the indicated θ values (c, 6-21G) and the keto forms shown in Fig. 1a (d, pm3). For clear comparison, the potentials in d are represented by the energy difference (ΔE) from the orthogonal conformation (global minimum).

was calculated the O \cdots H distance changes during rotation around the central C=C bond which is a key motion in TICT. As shown in Fig. 4b, the close coincidence between the model and the actual molecules supports that both model structures well represent the corresponding molecular set shown in Fig. 1. More importantly, a distinct difference between 5- and 6-membered compounds is observed, that is, the O \cdots H distances of 5-membered compounds are similar to or larger than the optimum value (1.80 Å, dotted horizontal line in Fig. 4b) at all the points during the rotation and the nearest to it at around a planar conformation, while the O \cdots H distances of 6-membered ones are smaller than the optimum value near the planar conformation and then cross it at a distorted conformation. From this, one can expect that intramolecular H bond would prefer a planar conformation for 5-membered compounds but rather tilt conformations for 6-membered ones. Such a different H-bonding behavior may differently modulate the net potential change during the TICT process from planar to orthogonal conformations.

Fig. 4c shows the S_1 -state rotational potential curves calculated for the two points of the model compound at the 6-21G level, where local energy wells near planar conformations are clearly seen by the effect of H-bond stabilization. As

expected, the 5-membered model ($\theta = 127^\circ$) exhibits a deep well of 7.69 kcal/mol because the planar conformation is the most stabilized due to the maximum H-bond strength, which is also the case for the actual 5-membered keto forms of HBO and HOXD (Fig. 4d).

On the contrary, the 6-membered model ($\theta = 111^\circ$) shows a shallow and rather blunt well (3.04 kcal/mol) due to the H-bond-preferred tilt structure. Note that, on the projection plane of O \cdots H distance and S_1 energy in Fig. 4a, the shorter-distance side of the optimum value shows the steeper destabilization, possibly giving rise to the less effect of H-bond stabilization on the TICT potential. This feature is more pronounced for the actual 6-membered molecules (Fig. 4d), so that local minima are distinguishably separated into two at ca. $\pm 15^\circ$ for HPQ and at ca. $\pm 10^\circ$ for HBP. As a net result of the different H-bond effect on TICT potential, 6-membered compounds have significantly lower rotational barrier than the 5-membered compounds. Based on this structure-dependent modulation of rotational barrier height, the tendency of ESIPt emission efficiency in Table 1 can be explained as follows: (1) 5-membered compounds have more efficient ESIPt emission from stable planar K^* formed just after ESIPt, due to the rather steep energy well deep enough to

block the fluorescence-quenching TICT reaction. (2) In the case of 6-membered compounds, the TICT reaction is a dominant decay path of the planar K^* due to the thermally accessible low energy barrier to orthogonal torsion, leading to the complete quenching of keto emission.

4. Conclusions

The tendency and efficiency of ESIPT emission for the representative ESIPT compounds has been theoretically investigated by the correlation of H-bond geometry factors with the energy barrier against the fluorescence-quenching TICT process. Elaborate calculations have shown that the structure (i.e., 5-membered versus 6-membered) of N-containing proton donor ring played a crucial role in intramolecular H-bond stabilization in the K^* state and thus determined the ESIPT emission differently.

Acknowledgment

This work was supported by the Korea Science and Engineering Foundation (KOSEF) through the National Research Lab. Program funded by the Ministry of Science and Technology (No. 2006-032246).

References

- [1] B. Strehmel, Fluorescence probes for material science, in: H.S. Nalwa (Ed.), *Advanced Functional Molecules and Polymers*, vol. 3, Gordon and Breach Science Publishers, 2001, p. 299.
- [2] J.R. Lakowicz, J. Malicka, I. Gryczynski, Z. Gryczynski, C.D. Geddes, *J. Phys. D: Appl. Phys.* 36 (2003) R240.
- [3] A.P. de Silva, N.D. McClenaghan, *Chem. Eur. J.* 8 (2002) 4935.
- [4] S. Kim, S.Y. Park, *Adv. Mater.* 15 (2003) 1341.
- [5] B.-K. An, S.-K. Kwon, S.-D. Jung, S.Y. Park, *J. Am. Chem. Soc.* 124 (2002) 14410.
- [6] J. Chen, C.C.W. Law, J.W.Y. Lam, Y. Dong, S.M.F. Lo, I.D. Williams, D. Zhu, B.Z. Tang, *Chem. Mater.* 15 (2003) 1535.
- [7] S.Y. Ryu, S. Kim, J. Seo, Y.-W. Kim, O.-H. Kwon, D.-J. Jang, S.Y. Park, *Chem. Commun.* (2004) 70.
- [8] D.W. Chang, S. Kim, S.Y. Park, H. Yu, D.-J. Jang, *Macromolecules* 33 (2000) 7223.
- [9] S. Kim, D.W. Chang, S.Y. Park, K. Kim, J.-I. Jin, *Bull. Korean Chem. Soc.* 22 (2001) 1407.
- [10] S. Kim, D.W. Chang, S.Y. Park, S.C. Jeoung, D. Kim, *Macromolecules* 35 (2002) 6064.
- [11] S. Kim, D.W. Chang, S.Y. Park, H. Kawai, T. Nagamura, *Macromolecules* 35 (2002) 2748.
- [12] S. Kim, S.Y. Park, I. Yoshida, H. Kawai, T. Nagamura, *J. Phys. Chem., Part B* 106 (2002) 9291.
- [13] F. Vollmer, W. Retig, *J. Photochem. Photobiol. A: Chem.* 95 (1996) 143.
- [14] M.I. Knyazhansky, A.V. Metelitsa, A.Ja. Bushkov, S.M. Aldoshin, *J. Photochem. Photobiol. A: Chem.* 97 (1996) 121.
- [15] W. Retig, *Angew. Chem. Int. Ed.* 25 (1986) 971.
- [16] O.K. Abou-Zied, R. Jimenez, E.H.Z. Thompson, D.P. Millar, F.E. Romesberg, *J. Phys. Chem. A* 106 (2002) 3665.
- [17] G. Gilli, F. Bellucci, V. Ferretti, V. Bertolasi, *J. Am. Chem. Soc.* 111 (1989) 1023.
- [18] G. Buemi, F.J. Zuccarello, *Mol. Struct. Theochem.* 581 (2002) 71.
- [19] A. Mordzinski, J. Lipkowski, G. Orzanowska, E. Tauer, *Chem. Phys.* 140 (1990) 167.
- [20] A.O. Doroshenko, E.A. Posokhov, A.A. Verezubova, L.M. Ptyagina, *J. Phys. Org. Chem.* 13 (2000) 253.